

Solar origin of heliospheric magnetic field inversions: evidence for coronal loop opening within pseudostreamers

Article

Accepted Version

Owens, M. J. ORCID: <https://orcid.org/0000-0003-2061-2453>, Crooker, N. U. and Lockwood, M. ORCID: <https://orcid.org/0000-0002-7397-2172> (2013) Solar origin of heliospheric magnetic field inversions: evidence for coronal loop opening within pseudostreamers. *Journal of Geophysical Research: Space Physics*, 118 (5). pp. 1868-1879. ISSN 2169-9402 doi: <https://doi.org/10.1002/jgra.50259> Available at <https://centaur.reading.ac.uk/32614/>

It is advisable to refer to the publisher's version if you intend to cite from the work. See [Guidance on citing](#).

Published version at: <http://dx.doi.org/10.1002/jgra.50259>

To link to this article DOI: <http://dx.doi.org/10.1002/jgra.50259>

Publisher: American Geophysical Union

All outputs in CentAUR are protected by Intellectual Property Rights law, including copyright law. Copyright and IPR is retained by the creators or other copyright holders. Terms and conditions for use of this material are defined in the [End User Agreement](#).

www.reading.ac.uk/centaur

CentAUR

Central Archive at the University of Reading

Reading's research outputs online

1 **Solar origin of heliospheric magnetic field inversions:**
2 **Evidence for coronal loop opening within**
3 **pseudostreamers**

M.J. Owens

4 Space Environment Physics Group, Department of Meteorology, University
5 of Reading, Earley Gate, PO Box 243, Reading RG6 6BB, UK

N.U. Crooker

6 Center for Space Physics, Boston University, Boston, MA 02215, USA

M. Lockwood

7 Space Environment Physics Group, Department of Meteorology, University
8 of Reading, Earley Gate, PO Box 243, Reading RG6 6BB, UK

M.J. Owens, Space Environment Physics Group, Department of Meteorology, University of Reading, Earley Gate, PO Box 243, Reading RG6 6BB, UK m.j.owens@reading.ac.uk

9 **Abstract.** The orientation of the heliospheric magnetic field (HMF) in
10 near-Earth space is generally a good indicator of the polarity of HMF foot
11 points at the photosphere. There are times, however, when the HMF folds
12 back on itself (is inverted), as indicated by suprathermal electrons moving
13 sunward while carrying the heat flux away from the Sun. Analysis of the near-
14 Earth solar wind during the period 1998-2011 reveals that inverted HMF is
15 present approximately . Inverted HMF is mapped to the coronal source sur-
16 face, where a new method is used to estimate coronal structure from the potential-
17 field source-surface model. We find a strong association with bipolar stream-
18 ers containing the heliospheric current sheet, as expected, but also with unipo-
19 lar or pseudostreamers, which contain no current sheet. Because large-scale
20 inverted HMF is a widely-accepted signature of interchange reconnection at
21 the Sun, this finding provides strong evidence for models of the slow solar
22 wind which involve coronal loop opening by reconnection within pseudostreamer
23 belts as well as the bipolar streamer belt. Occurrence rates of bipolar- and
24 pseudostreamers suggest that they are equally likely to result in inverted HMF
25 and, therefore, presumably undergo interchange reconnection at approximately
26 the same rate. Given the different magnetic topologies involved, this suggests
27 the rate of reconnection is set externally, possibly by the differential rota-
28 tion rate which governs the circulation of open solar flux.

1. Introduction

29 large-scale heliospheric magnetic field (HMF) is generally well described by the Parker
30 spiral. $135^\circ/315^\circ$ for outward/inward polarity HMF [e.g., *Borovsky, 2010*]. The helio-
31 spheric current sheet (HCS) separates sectors of inward and outward magnetic flux and
32 projects back to a coronal source-surface as a neutral line marking the heliomagnetic
33 equator. Crossings of the near-Earth HCS can be identified by rapid changes in the HMF
34 direction from 135° to 315° , or vice versa. This is shown schematically in Figure 1a.

35 HMF connectivity to the Sun can usually be inferred by suprathermal electron (STE)
36 observations. Open HMF, which has one end connected to the Sun, exhibits an adiabati-
37 cally focussed STE beam, or "strahl," that originates in the solar corona [*Feldman et al.,*
38 *1975; Rosenbauer et al., 1977*]. Thus outward (inward) magnetic sectors should contain a
39 strahl which is parallel (antiparallel) to the HMF, as shown in Figure 1a. , when both par-
40 allel and antiparallel strahls are present, reveal "closed" HMF, with both ends of the field
41 line connected to the Sun (times 2 and 3 in Figure 1b). They are strongly associated with
42 interplanetary coronal mass ejections [*Gosling et al., 1987; Wimmer-Schweingruber et al.,*
43 *2006*], which in turn are frequently encountered at magnetic sector boundaries [*Crooker*
44 *et al., 1998*, see also Figure 1b].

45 There also exist periods with a single strahl in the opposite sense to that expected from
46 the magnetic field direction [*Kahler and Lin, 1994, 1995; Kahler et al., 1996; Crooker*
47 *et al., 1996; Crooker et al., 2004b*], as shown in Figures 1c-e. These intervals imply that
48 the magnetic field is folded back upon itself, or inverted. Inverted HMF intervals can be
49 bounded by a change in the magnetic field direction with no change in the strahl direction

50 and vice versa. Pairs of the former are common and can be found both near the HCS,
51 as in Figure 1c, and in unipolar regions [e.g., *Balogh et al.*, 1999], as in Figure 1d. These
52 pairs of field changes bound inversions that are usually of short duration, on the order
53 of an hour or two. In contrast, inversions bounded on at least one side by a change in
54 the strahl direction with no change in the magnetic field direction are less common but
55 can be of long duration, on the order of a day or more [*Crooker et al.*, 2004b]. Moreover,
56 they can only be understood in terms of a three-dimensional structure. In cases involving
57 the HCS, as in Figure 1e, where the dashed field lines lie out of the plane of the Figure,
58 the inversion results in a mismatch between the magnetic and electron signatures of the
59 sector boundary [*Crooker et al.*, 2004b].

60 While some of the smaller inversions may be the product of large-scale turbulent pro-
61 cesses, the larger inversions appear to be robust signatures of near-Sun magnetic inter-
62 change reconnection, as sketched in Figures 1c-e, where a green X marks a reconnection
63 site. The legs of large loops expanding into the heliosphere reconnect with adjacent open
64 field lines. *Crooker et al.* [2004b] suggest that the expanding loops are at the quiet end
65 of a spectrum of large-scale transient outflows, with coronal mass ejections (CMEs) at
66 the active end. This interpretation is supported by the observation of coronal inflows
67 and collapsing loops at locations where the HCS is inclined to the solar rotation direction
68 [*Sheeley and Wang*, 2001], taken to be signatures of magnetic reconnection. The asso-
69 ciation of inverted HMF with the HCS suggests the solar origin of the expanding loops
70 can be bipolar helmet streamers which surround the coronal source-surface neutral line
71 and separate magnetic flux from coronal holes of opposite magnetic polarity, e.g., the

72 two polar coronal holes at solar minimum. This paper also considers unipolar streamers,
73 called "pseudostreamers," as an additional source.

74 Pseudostreamers are very similar to bipolar streamers in coronagraph observations.
75 They are also formed at the boundary between coronal magnetic flux from two different
76 coronal holes, but unlike bipolar streamers, the flux at both foot points is of the same
77 polarity and, thus, they do not contain current sheets [e.g., *Eselevich*, 1998; *Eselevich*
78 *et al.*, 1999; *Zhao and Webb*, 2003; *Wang et al.*, 2007]. There has recently been much
79 interest in pseudostreamers as a possible source of the slow solar wind [*Crooker et al.*,
80 2012; *Riley and Luhmann*, 2012], either through the expansion of coronal magnetic flux
81 tubes [*Wang et al.*, 2012], or through the intermittent release of plasma by the opening
82 of coronal loops via magnetic reconnection [*Antiochos et al.*, 2011]. *Crooker et al.* [2012]
83 demonstrate that pseudostreamers occur in belts which are topologically connected to the
84 bipolar streamer belt, thus forming a network of slow solar wind sources.

85 In this study we investigate the properties and solar origin of inverted heliospheric mag-
86 netic flux during the period 1998 to 2011, for which almost continuous HMF and STE data
87 are available from the Advanced Composition Explorer (ACE) spacecraft. In particular,
88 comparisons are made with the locations of bipolar and pseudostreamers estimated using
89 the potential-field source-surface (PFSS) model of the corona.

2. Detection of HMF inversions

90 The 272eV energy channel is used, as it is well within the suprathermal range, showing
91 little contribution from the core electron population, but still providing high count rates
92 [e.g., *Anderson et al.*, 2012]. The SWEPAM PAD data are available from January 1998
93 to August 2011, which determines the interval used in this study.

94 discriminate between closed HMF and 90° pitch-angle depletions owing to mirroring
95 from large-scale, downstream structures [*Gosling et al.*, 2001], so closed flux occurrence is
96 likely overestimated. Furthermore, while counterstreaming electron intervals are separated
97 out from inverted and uninverted flux, no attempt is made to explicitly exclude ICMEs.
98 Indeed, if ICMEs contain "open" inverted field lines, they must result from reconnection
99 in the corona in the same way as ambient solar wind intervals [*Owens and Crooker*,
100 2006, 2007]. By including all solar wind data in the study, no assumptions are made
101 about the source and processes involved in the creation of inverted HMF.

102 There are

3. Properties of HMF inversions

103 Figure 3 shows the probability distribution functions (PDFs) of solar wind parameters.
104 . The solar wind properties of

4. Association with bipolar and pseudostreamers

105 Thus to aid in the interpretation of these data, we use a potential-field source-surface
106 (PFSS) model of the corona [*Schatten et al.*, 1969] based on WSO magnetograms to
107 identify the locations of the HCS and, hence, bipolar streamers as well as pseudostreamers.

4.1. Case studies

108 The pink and light grey regions show, respectively, outward and inward polarity coronal
109 holes, i.e., the photospheric foot points of magnetic field lines reach the source surface at
110 2.5 solar radii. Red (white) lines show the . Overlaid on the ecliptic plane is the observed
111 magnetic polarity in near-Earth space, ballistically mapped back to the source surface
112 using the observed solar wind speed, with red/white dots indicating , as determined in

113 Section 2. For this particular Carrington rotation, there is agreement between the mag-
114 netic polarity predicted by the PFSS model and that observed near-Earth. Green crosses
115 show the coronal source-surface locations of observed HMF inversions at the heliographic
116 latitude of Earth.

117 The two intervals of inverted HMF at Carrington longitude of . The remaining HMF
118 inversions are also associated with a change in magnetic connectivity, with the photo-
119 spheric foot points along Earth orbit shifting between different coronal holes, but without
120 an associated change in foot point polarity, indicative of pseudostreamers. These HMF
121 inversions are thus associated with pseudostreamers rather than bipolar streamers.

122 define a parameter dS , the distance between photospheric foot points of neighbouring
123 points on the source surface. In practice, the magnitude of dS will depend on the spatial
124 resolution at which field lines are traced, making units somewhat arbitrary. In this study,
125 we calculate dS by moving along the ecliptic plane in 1° steps. When adjacent points on
126 the source surface map to the same coronal hole, dS will be small, for example as seen
127 between 0° and 60° Carrington longitude for CR1990. When neighbouring source-surface
128 points map to different coronal holes, however, such as the HCS crossing at 310° Carring-
129 ton longitude, dS will be very large. The middle panel of Figure 4 shows $\log_e(dS)$ as a
130 function of Carrington longitude along the ecliptic plane. Vertical yellow lines mark HCS
131 crossings, where $\log_e(dS)$ spikes correspond to bipolar streamers. The dashed horizontal
132 line at $\log_e(dS) = 3$ marks the threshold selected to define a streamer. It is the value
133 which $\log_e(dS)$ reaches or exceeds at all HCS crossings in the 1998 to 2011 period and
134 corresponds to source surface points with a 1° separation having a photospheric footpoint
135 separation of $\geq 5^\circ$. It thus selects all bipolar streamers and appears to select most sig-

136 nificant pseudostreamers while suppressing smaller structures. Blue vertical lines mark
137 $\log_e(dS)$ spikes without polarity reversals, our definition of a pseudostreamer. The 17
138 1-hour intervals of inverted HMF not associated with the HCS in CR1990 all map close
139 to the longitudes of pseudostreamers.

140 The bottom panel of Figure 4 is a contour plot of dS at all latitudes. It demonstrates
141 in another way the finding reported by [Crooker *et al.*, 2012] that pseudostreamer belts
142 , but connect to the bipolar streamer belt to form a network of slow solar wind sources
143 that expands to cover the source surface during solar maximum. As is the case for bipolar
144 streamers, HMF inversions are not associated with all pseudostreamers; however, Figure
145 4 demonstrates that streamer-associated inverted HMF is likely to be common at all
146 latitudes near solar maximum.

4.2. Statistical analysis

147 In order to systematically analyse the entire 1998-2011 interval, and define strict thresh-
148 olds for association between inverted HMF and streamers. We begin by including only
149 Carrington rotations in which the PFSS model provides a reasonable representation of
150 the observed magnetic structure of the corona and solar wind. By assigning +1 (-1) to
151 outward (inward) Parker spiral polarity, and ignoring undetermined, counterstreaming
152 and inverted intervals, we compute the mean-square error (MSE) between the PFSS and
153 observed sector structure mapped to the source surface. Thus MSE is a combination of
154 errors in the PFSS solution and errors in the simple ballistic mapping of near-Earth solar
155 wind to the coronal source surface.

156 of ecliptic longitudes are covered by pseudostreamers (bipolar streamers). Note that the
157 association scheme allows a single inverted HMF interval to map to both a bipolar and
158 pseudostreamer if they are located close in longitude. Table 2 summarises these results.

159 In general, there are insufficient inverted HMF events to detect significant differences in
160 the of solar wind properties of bipolar- and pseudostreamer-associated inversions. Prob-
161 ability distributions of density, however (not shown), suggest that HMF inversions from
162 bipolar streamers contain denser solar wind than inverted HMF from pseudostreamers,
163 consistent with general properties of pseudostreamer-associated solar wind [*Wang et al.*,
164 2012].

5. Conclusions and Discussion

165 The polarity of the photospheric foot point of heliospheric magnetic flux (HMF) can
166 be independently estimated from both the local HMF orientation, as measured using in
167 situ magnetometer observations, and the direction of the suprathermal electron beam,
168 or "strahl." For the bulk of the solar wind, these two methods show agreement. There
169 are intervals, however, in which the strahl is directed towards the Sun, implying that the
170 magnetic field line is inverted, or folded back on itself. This is an expected signature of
171 near-Sun magnetic reconnection by which the Sun can open previously closed heliospheric
172 loops [*Owens et al.*, 2011; *Owens and Lockwood*, 2012]. Using an automated data analysis
173 method, we find inverted flux in approximately 5.5% of the solar wind data between 1998
174 and 2011, though this is likely an underestimate due to strict selection criteria. We do
175 not find a strong solar cycle variation in the occurrence rate of inverted HMF, but this
176 finding is confined to the ecliptic plane . Inverted HMF is associated with dense, slow,
177 cool solar wind, with lower than average magnetic field intensity. In order to determine

178 the solar origin of these structures, we used a potential-field source-surface model to
179 infer the global structure of the coronal magnetic field and a new automated detection
180 method for bipolar and pseudostreamers. Of the 2263 1-hour inverted HMF intervals
181 identified in the solar wind and mapped back to the coronal source surface, 1310 (58%)
182 are associated with streamers. Given that the probability of a solar wind interval being
183 associated with a streamer by chance is 52%, the association between inverted HMF
184 and streamers is significant at the 99.9% level. Of the 1310 streamer-associated inverted
185 HMF intervals, 949 (504) map to pseudostreamers (bipolar streamers). This ratio is in
186 reasonable agreement with the occurrence rates of pseudostreamers and bipolar streamers
187 in the ecliptic plane, 39% and 20%, respectively,

188 If we assume that inverted HMF is primarily a signature of reconnection in the corona
189 [e.g., *Titov et al.*, 2011], our results suggest that the rate of reconnection is similar within
190 bipolar and pseudostreamers. This seems reasonable in view of their magnetic structure.
191 For the bipolar streamer case, a three-dimensional magnetic configuration for interchange
192 reconnection that can create the inversion is illustrated in 1e and has already been dis-
193 cussed in section 1. For the pseudostreamer case, an appropriate magnetic configuration
194 can be drawn in just two dimensions, as illustrated in Figure 6. Closed loops within one
195 of the two arcades that form pseudostreamers are shown to rise as a result of photospheric
196 flux emergence, but could equally be the result of loop foot point shearing, etc. In the
197 top panel, the rising loop undergoes interchange reconnection before it reaches the solar
198 wind acceleration height and therefore doesn't result in the generation of inverted HMF.
199 This configuration is common from the solar perspective [e.g., *Wang et al.*, 2007; *Crooker*
200 *et al.*, 2012]. In contrast, from the heliospheric perspective, the rising loops are dragged

201 out by the solar wind before interchange reconnection takes place, which does generate
202 inverted HMF, as illustrated in the bottom panels. Thus pseudostreamer loop expansion
203 and opening via interchange reconnection would transport pre-existing open solar flux in
204 much the same way as the CME-driven transport proposed by *Owens et al.* [2007]. Indeed,
205 as proposed by *Crooker et al.* [2004b] for loops expanding from the helmet arcade in the
206 case of bipolar streamers, loops that create inversions from pseudostreamers can also be
207 considered as the quiet end of a spectrum of loops, where the active end is CMEs. This
208 analogy holds because pseudostreamers are well-documented sources of CMEs [*Fainshtein,*
209 *1997; Eselevich et al., 1999; Zhao and Webb, 2003; Liu and Hayashi, 2006*].

210 In addition, similar levels of association between inverted HMF with bipolar and pseu-
211 dostreamers, despite the differing magnetic topologies, suggest that the reconnection rate
212 is externally controlled. One possibility is the stress between the differential rotation of
213 the photosphere and the rigid corotation of the corona [*Nash et al., 1988; Wang and Shee-*
214 *ley, 2004*] and the consequent circulation of open solar flux [*Fisk et al., 1999; Fisk and*
215 *Schwadron, 2001*]. We note that inverted HMF is the expected heliospheric signature of
216 large coronal loop opening, one of the proposed mechanisms for slow solar wind formation
217 [e.g., *Fisk, 2003*]. Thus our results provide support for the idea of pseudostreamers being
218 a source of slow solar wind through intermittent release from previously closed coronal
219 loops [*Antiochos et al., 2011*], though the effect of magnetic flux tube expansion [*Wang*
220 *et al., 2012*] may still be important.

221 Inverted HMF has direct implications for in situ spacecraft estimates of the total mag-
222 netic flux threading the solar source surface, often referred to as the unsigned open solar
223 flux, OSF [e.g., *Owens et al., 2008a*]. Figures 1c and 1d clearly illustrate the issue: In-

224 verted HMF provides magnetic flux which threads the heliocentric sphere at 1 AU, but
225 does not map back to the source surface, resulting in an overestimate in OSF from in
226 situ observations. , decomposing the HMF along the Parker spiral direction, which can
227 successfully remove the effects of waves and turbulence [Erdős and Balogh, 2012], may
228 not address this particular issue. Both the occurrence rate and magnetic field strength
229 associated with inverted HMF are small, suggesting this may not have a large effect on
230 OSF estimates. Even if inverted HMF has an average magnetic flux density as high as
231 the rest of the solar wind, the decrease in the unsigned OSF would only be $2 \times 5\% = 10\%$.
232 The factor 2 arises as follows: if inverted HMF intervals contain ϕ_I of magnetic flux, the
233 unsigned OSF will be overestimated by $2\phi_I$, since both the inverted and "return" flux
234 thread the heliocentric surface but not the coronal source surface. We note that, in gen-
235 eral, inverted HMF intervals are less than a day long, though this may be partly due to
236 the strict criteria used and the time interval considered [c.f. Crooker et al., 2004b]. Thus
237 taking 1-day averages of the radial magnetic field for the purposes of estimating OSF
238 may indirectly negate the effect of inverted HMF [c.f. Wang and Sheeley, 1995], though
239 it does not directly address the issue of physical origin [see also Lockwood et al., 2009, for
240 discussion of correction of 1-AU measurements to the coronal source surface].

241 In summary, we have developed a new method for identifying bipolar streamers and
242 pseudostreamers in PFSS synoptic maps. The results confirm that together these struc-
243 tures form a network of slow solar wind sources which expands over the source surface at
244 solar maximum. Moreover, we have analyzed suprathermal electron data from the solar
245 wind and find that, like bipolar streamers, pseudostreamers are sources of HMF inversions.
246 These are understood to be signatures of coronal loops that expand into the heliosphere

247 and subsequently become open through reconnection in the corona. Loop-opening is a
248 key process in one of two competing models for the source of the slow wind.

249 **Acknowledgments.** We are grateful to the ACE Science Center (ASC) for magnetic
250 field and suprathermal electron data, and to T. Hoeksema of Stanford University for
251 WSO magnetograms. Research for this paper was supported in part (NUC) by the U.S.
252 National Science Foundation under grant AGS-0962645. This work was facilitated by
253 the ISSI workshop 233, "Long-term reconstructions of solar and solar wind parameters"
254 organised by L. Svalgaard, E. Cliver, J. Beer and M. Lockwood. MO thanks Andre Balogh
255 of Imperial College London for useful discussions.

References

- 256 Anderson, B. R., R. M. Skoug, J. T. Steinberg, and D. J. McComas, Variability of
257 the solar wind suprathermal electron strahl, *J. Geophys. Res.*, *117*, A04107, doi:
258 10.1029/2011JA017269, 2012.
- 259 Antiochos, S. K., Z. Mikić, V. S. Titov, R. Lionello, and J. A. Linker, A Model
260 for the Sources of the Slow Solar Wind, *Astrophys. J.*, *731*, 112, doi:10.1088/0004-
261 637X/731/2/112, 2011.
- 262 Balogh, A., R. J. Forsyth, E. A. Lucek, T. S. Horbury, and E. J. Smith, Heliospheric
263 magnetic field polarity inversions at high heliographic latitudes, *Geophys. Res. Lett.*,
264 *26*, 631–634, doi:10.1029/1999GL900061, 1999.
- 265 Borovsky, J. E., On the variations of the solar wind magnetic field about the Parker spiral
266 direction, *J. Geophys. Res.*, *115*, A09101, doi:10.1029/2009JA015040, 2010.
- 267 Crooker, N. U., M. E. Burton, G. L. Siscoe, S. W. Kahler, J. T. Gosling, and E. J.

268 Smith, Solar wind streamer belt structure, *J. Geophys. Res.*, *101*, 24,331–24,342, doi:
269 10.1029/96JA02412, 1996.

270 Crooker, N. U., J. T. Gosling, and S. W. Kahler, Magnetic clouds at sector boundaries,
271 *J. Geophys. Res.*, *103*, 301, 1998.

272 Crooker, N. U., C.-L. Huang, S. M. Lamassa, D. E. Larson, S. W. Kahler, and
273 H. E. Spence, Heliospheric plasma sheets, *J. Geophys. Res.*, *109*, A03107, doi:
274 10.1029/2003JA010170, 2004a.

275 Crooker, N. U., S. W. Kahler, D. E. Larson, and R. P. Lin, Large-scale magnetic field in-
276 versions at sector boundaries, *J. Geophys. Res.*, *109*, doi:10.1029/2003JA010278, 2004b.

277 Crooker, N. U., S. K. Antiochos, X. Zhao, and M. Neugebauer, Global network of slow
278 solar wind, *J. Geophys. Res.*, *117*, A04104, doi:10.1029/2011JA017236, 2012.

279 Erdős, G., and A. Balogh, Magnetic Flux Density Measured in Fast and Slow Solar Wind
280 Streams, *Astrophys. J.*, *753*, 130, doi:10.1088/0004-637X/753/2/130, 2012.

281 Eselevich, V. G., On the structure of coronal streamer belts, *J. Geophys. Res.*, *103*, 2021,
282 doi:10.1029/97JA02365, 1998.

283 Eselevich, V. G., V. G. Fainshtein, and G. V. Rudenko, Study of the structure of streamer
284 belts and chains in the solar corona, *188*, 277–297, 1999.

285 Fainshtein, V. G., An Investigation of Solar Factors Governing Coronal Mass Ejection
286 Characteristics, *174*, 413–435, 1997.

287 Feldman, W. C., J. R. Asbridge, S. J. Bame, M. D. Montgomery, and S. P. Gary, Solar
288 wind electrons, *J. Geophys. Res.*, *80*, 4181–4196, 1975.

289 Fisk, L. A., Acceleration of the solar wind as a result of the reconnection of open magnetic
290 flux with coronal loops, *J. Geophys. Res.*, *108*, 1157, doi:10.1029/2002JA009284, 2003.

291 Fisk, L. A., and N. A. Schwadron, The behaviour of the open magnetic field of the Sun,
292 *Astrophys. J.*, *560*, 425–438, 2001.

293 Fisk, L. A., T. H. Zurbuchen, and N. A. Schwadron, Coronal hole boundaries and their
294 interaction with adjacent regions, *Space Sci. Rev.*, *87*, 43–54, 1999.

295 Garrard, T. L., A. J. Davis, J. S. Hammond, and S. R. Sears, The ACE Science Center,
296 *Space Sci. Rev.*, *86*, 649–663, doi:10.1023/A:1005096317576, 1998.

297 Gosling, J. T., D. N. Baker, S. J. Bame, W. C. Feldman, and R. D. Zwickl, Bidirectional
298 solar wind electron heat flux events, *J. Geophys. Res.*, *92*, 8519–8535, 1987.

299 Gosling, J. T., S. J. Bame, W. C. Feldman, D. J. McComas, J. L. Phillips, and B. E. Gold-
300 stein, Counterstreaming suprathermal electron events upstream of corotating shocks in
301 the solar wind beyond approximately 2 AU: ULYSSES, *Geophys. Res. Lett.*, *20*, 2335–
302 2338, doi:10.1029/93GL02489, 1993.

303 Gosling, J. T., R. M. Skoug, and W. C. Feldman, Solar wind electron halo depleeetions at
304 90-degree pitch angle, *Geophys. Res. Lett.*, *28*, 4155–4158, doi:10.1029/2001GL013758,
305 2001.

306 Gosling, J. T., R. M. Skoug, D. J. McComas, and C. W. Smith, Magnetic disconnection
307 from the sun: Observations of a reconnection exhaust in the solar wind at the he-
308 liospheric current sheet, *Geophys. Res. Lett.*, *32*, L05,105, doi:10.1029/2005GL022406,
309 2005.

310 Gosling, J. T., S. Eriksson, D. J. McComas, T. D. Phan, and R. M. Skoug, Multiple
311 magnetic reconnection sites associated with a coronal mass ejection in the solar wind,
312 *J. Geophys. Res.*, *112*, 8106–+, doi:10.1029/2007JA012418, 2007.

313 Haggerty, D. K., E. C. Roelof, C. W. Smith, N. F. Ness, R. L. Tokar, and R. M. Skoug,
314 Interplanetary magnetic field connection to the L1 Lagrangian orbit during upstream
315 energetic ion events, *J. Geophys. Res.*, *105*, 25,123–25,132, doi:10.1029/1999JA000346,
316 2000.

317 Hammond, C. M., W. C. Feldman, D. J. McComas, J. L. Phillips, and R. J. Forsyth,
318 Variation of electron-strahl width in the high-speed solar wind: ULYSSES observations,
319 *Astron. Astrophys.*, *316*, 350–354, 1996.

320 Hapgood, M. A., G. Bowe, M. Lockwood, D. M. Willis, and Y. Tulunay, Variability of the
321 interplanetary magnetic field at 1 A.U. over 24 years: 1963-1986, *Planet. Space Sci.*,
322 *39*, 411–423, doi:10.1016/0032-0633(91)90003-S, 1991.

323 Kahler, S., and R. P. Lin, The determination of interplanetary magnetic field polarities
324 around sector boundaries using E greater than 2 keV electrons, *Geophys. Res. Lett.*, *21*,
325 1575–1578, doi:10.1029/94GL01362, 1994.

326 Kahler, S., N. U. Crooker, and J. T. Gosling, Properties of interplanetary magnetic sector
327 boundaries based on electron heat-flux flow directions, *J. Geophys. Res.*, *103*, 20,603–
328 20,612, doi:10.1029/98JA01745, 1998.

329 Kahler, S. W., and R. P. Lin, An Examination of Directional Discontinuities and Magnetic
330 Polarity Changes around Interplanetary Sector Boundaries Using $E > 2$ keV Electrons,
331 *Sol. Phys.*, *161*, 183–195, doi:10.1007/BF00732092, 1995.

332 Kahler, S. W., N. U. Crooker, and J. T. Gosling, The topology of intrasector rever-
333 sals of the interplanetary magnetic field, *J. Geophys. Res.*, *101*, 24,373–24,382, doi:
334 10.1029/96JA02232, 1996.

335 Liu, Y., and K. Hayashi, The 2003 October–November Fast Halo Coronal Mass Ejections
336 and the Large-Scale Magnetic Field Structures, *Astrophys. J.*, *640*, 1135–1141, doi:
337 10.1086/500290, 2006.

338 Lockwood, M., M. Owens, and A. P. Rouillard, Excess open solar magnetic flux from
339 satellite data: 2. A survey of kinematic effects, *J. Geophys. Res.*, *114*, A11104, doi:
340 10.1029/2009JA014450, 2009.

341 McComas, D. J., J. T. Gosling, D. Winterhalter, and E. J. Smith, Interplanetary magnetic
342 field draping about fast coronal mass ejecta in the outer heliosphere, *J. Geophys. Res.*,
343 *93*, 2519–2526, doi:10.1029/JA093iA04p02519, 1988.

344 McComas, D. J., S. J. Bame, B. S. J., W. C. Feldman, J. L. Phillips, P. Riley, and
345 J. W. Griffee, Solar wind electron proton alpha monitor (SWEPAM) for the Advanced
346 Composition Explorer, *Space Sci. Rev.*, *86*, 563, 1998.

347 Nash, A. G., N. R. Sheeley, Jr., and Y.-M. Wang, Mechanisms for the rigid rotation of
348 coronal holes, *Sol. Phys.*, *117*, 359–389, 1988.

349 Owens, M. J., and P. J. Cargill, Non-radial solar wind flows induced by the motion of
350 interplanetary coronal mass ejections, *Ann. Geophys.*, *22*, 4397–4395, 2004.

351 Owens, M. J., and N. U. Crooker, Coronal mass ejections and magnetic flux buildup in
352 the heliosphere, *J. Geophys. Res.*, *111*, A10104, doi:10.1029/2006JA011641, 2006.

353 Owens, M. J., and N. U. Crooker, Reconciling the electron counterstreaming and dropout
354 occurrence rates with the heliospheric flux budget, *J. Geophys. Res.*, *112*, A06106, doi:
355 10.1029/2006JA012159, 2007.

356 Owens, M. J., and M. Lockwood, Cyclic loss of open solar flux since 1868: The link
357 to heliospheric current sheet tilt and implications for the Maunder Minimum, *J. Geo-*

358 *phys. Res.*, 117, A04102, doi:10.1029/2011JA017193, 2012.

359 Owens, M. J., N. A. Schwadron, N. U. Crooker, W. J. Hughes, and H. E. Spence, Role of
360 coronal mass ejections in the heliospheric Hale cycle, *Geophys. Res. Lett.*, 34, L06104,
361 doi:10.1029/2006GL028795, 2007.

362 Owens, M. J., C. N. Arge, N. U. Crooker, N. A. Schwadron, and T. S. Horbury, Esti-
363 mating total heliospheric magnetic flux from single-point in situ measurements, *J. Geo-*
364 *phys. Res.*, 113, A12103, doi:10.1029/2008JA013677, 2008a.

365 Owens, M. J., N. U. Crooker, N. A. Schwadron, T. S. Horbury, S. Yashiro, H. Xie, O. C. St
366 Cyr, and N. Gopalswamy, Conservation of open solar magnetic flux and the floor in the
367 heliospheric magnetic field, *Geophys. Res. Lett.*, L20108, doi:10.1029/2008GL035813,
368 2008b.

369 Owens, M. J., N. U. Crooker, and M. Lockwood, How is open solar magnetic flux lost
370 over the solar cycle?, *J. Geophys. Res.*, 116, A04111, doi:10.1029/2010JA016039, 2011.

371 Phan, T. D., et al., A magnetic reconnection X-line extending more than 390 Earth radii
372 in the solar wind, *Nature*, 439, 175–178, doi:10.1038/nature04393, 2006.

373 Richardson, I. G., and H. V. Cane, Near-earth solar wind flows and related geomagnetic
374 activity during more than four solar cycles (1963-2011), *J. Geophys. Res.*, 2(26), A02,
375 doi:10.1051/swsc/2012003, 2012.

376 Riley, P., and J. G. Luhmann, Interplanetary Signatures of Unipolar Streamers and the
377 Origin of the Slow Solar Wind, *Sol. Phys.*, 277, 355–373, doi:10.1007/s11207-011-9909-0,
378 2012.

379 Rosenbauer, H., et al., A survey on initial results of the HELIOS plasma experiment,
380 *Journal of Geophysics Zeitschrift Geophysik*, 42, 561–580, 1977.

381 Schatten, K. H., J. M. Wilcox, and N. F. Ness, A model of interplanetary and coronal
382 magnetic fields, *Sol. Phys.*, *9*, 442–455, 1969.

383 Sheeley, N. R., Jr., and Y.-M. Wang, Coronal Inflows and Sector Magnetism, *Astro-*
384 *phys. J. Lett.*, *562*, L107–L110, doi:10.1086/338104, 2001.

385 Smith, C. W., J. L’Heureux, N. F. Ness, M. H. Acuna, L. F. Burlaga, and J. Scheifele,
386 The ACE magnetic fields experiment, *Space Sci. Rev.*, *86*, 613, 1998.

387 Steinberg, J. T., J. T. Gosling, R. M. Skoug, and R. C. Wiens, Suprathermal electrons in
388 high-speed streams from coronal holes: Counterstreaming on open field lines at 1 AU,
389 *J. Geophys. Res.*, *110*, A06103, doi:10.1029/2005JA011027, 2005.

390 Titov, V. S., Z. Mikić, J. A. Linker, R. Lionello, and S. K. Antiochos, Magnetic Topology
391 of Coronal Hole Linkages, *Astrophys. J.*, *731*, 111, doi:10.1088/0004-637X/731/2/111,
392 2011.

393 Wang, Y., and N. R. Sheeley, Jr., Footpoint Switching and the Evolution of Coronal
394 Holes, *Astrophys. J.*, *612*, 1196–1205, doi:10.1086/422711, 2004.

395 Wang, Y.-M., and N. R. Sheeley, Jr., Solar Implications of ULYSSES Interplanetary Field
396 Measurements, *Astrophys. J. Lett.*, *447*, L143–L146, doi:10.1086/309578, 1995.

397 Wang, Y.-M., N. R. Sheeley, Jr., and N. B. Rich, Coronal Pseudostreamers, *Astrophys. J.*,
398 *658*, 1340–1348, doi:10.1086/511416, 2007.

399 Wang, Y.-M., R. Grappin, E. Robbrecht, and N. R. Sheeley, Jr., On the Nature of the
400 Solar Wind from Coronal Pseudostreamers, *Astrophys. J.*, *749*, 182, doi:10.1088/0004-
401 637X/749/2/182, 2012.

402 Wimmer-Schweingruber, R. F., et al., Understanding interplanetary coronal mass ejection
403 signatures, *Space Sci. Rev.*, *123*, 177–216, doi:10.1007/s11214-006-9017-x, 2006.

404 Zhao, X. P., and D. F. Webb, Source regions and storm effectiveness of frontside full halo
405 coronal mass ejections, *J. Geophys. Res.*, *108*, 1234, doi:10.1029/2002JA009606, 2003.

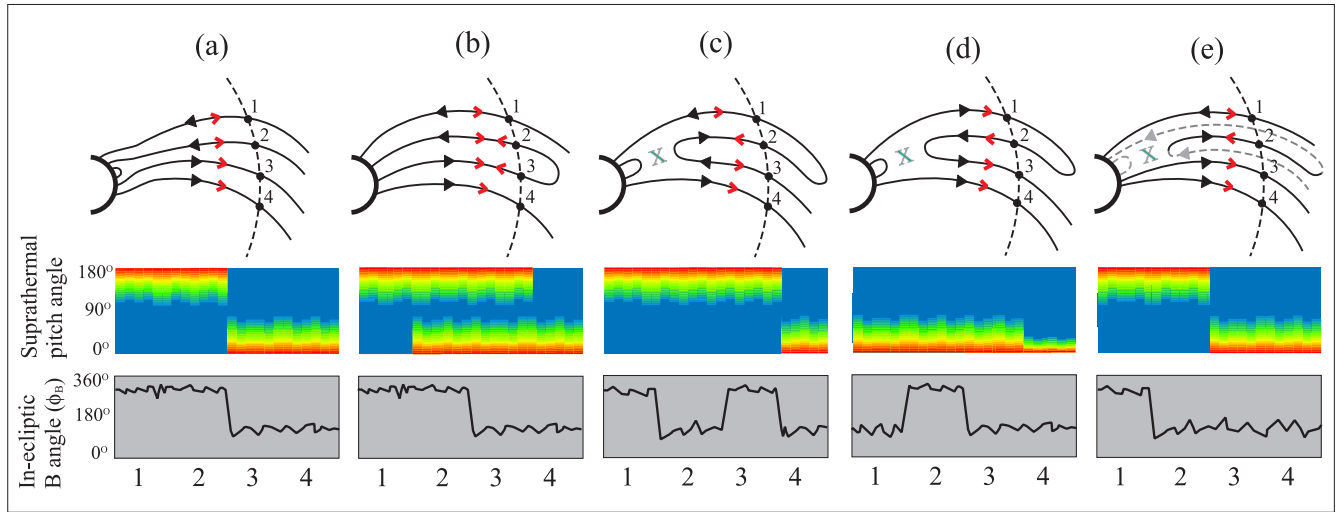


Figure 1. Sketches of possible HMF configurations and the resulting magnetic field and suprathermal electron signatures in near-Earth space. Red (black) arrows show the suprathermal electron strahl (magnetic field polarity), while green crosses show the position of magnetic reconnection. (a) A typical sector boundary/HCS crossing. (b) A sector boundary accompanied by closed HMF loops, likely part of an ICME. (c) A sector boundary/HCS crossing containing an inverted HMF interval at time 2. (d) An inverted HMF interval at time 2 embedded within a unipolar region. (e) A sector boundary with mismatched electron and magnetic signatures. The dashed lines show portions of the inverted HMF structure which are out of the ecliptic plane and not encountered by the observing spacecraft [after *Crooker et al.*, 2004b].

		# 1-hour intervals	% of available data
Magnetometer	Sunward HMF	53714	44.9%
Data	Antisunward HMF	56684	47.3%
	Undetermined	9366	7.83%
	Inward sector	60252	50.4%
	Outward sector	59041	49.3%
	Undetermined	371	0.31%
Suprathermal	Parallel strahl	37961	31.7%
electron data	Antiparallel strahl	37774	31.6%
	Counterstreaming	17023	14.2%
	Undetermined	26906	22.5%
Combined	Uninverted	57345	48.0%
datasets	Inverted	6608	5.53%
	Counterstreaming	19388	16.2%
	Undetermined	36139	30.2%

Table 1. The number of 1-hour observation periods of different HMF populations obtained using the magnetic field and suprathermal electron selection criteria.

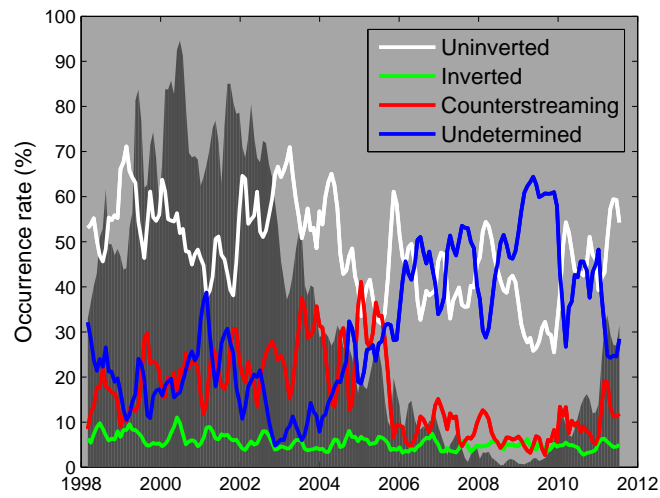


Figure 2. Three-Carrington rotation averages of the occurrence rates of various HMF topologies as a function of time. Sunspot number, scaled to fit the axis, is shown as the dark shaded region. Although some changes in the various HMF populations are likely to be due to changes in the electron detector, what this figure makes clear is that inverted flux is detected throughout the solar cycle.

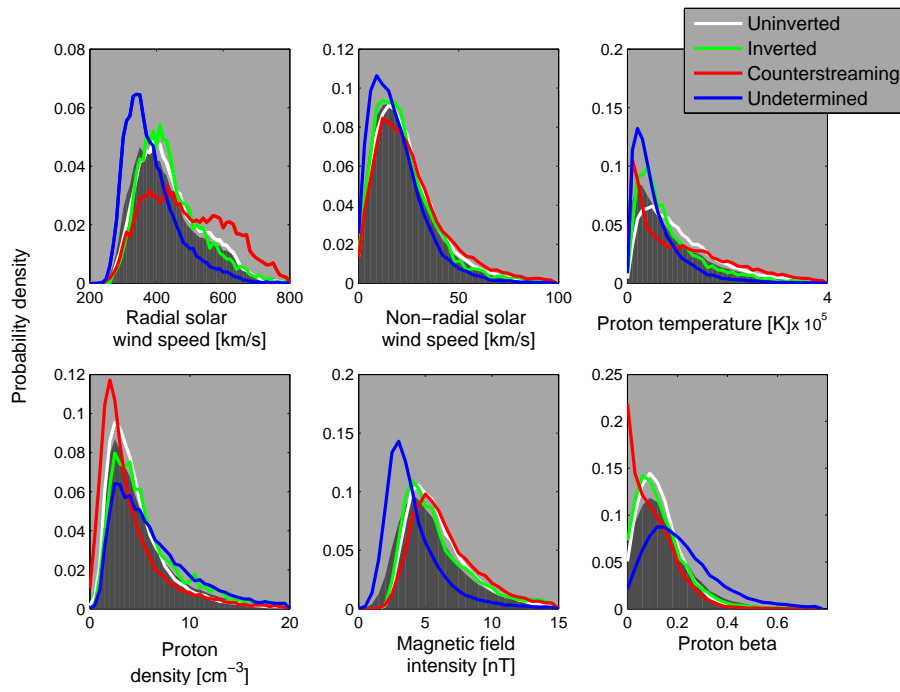


Figure 3. Probability distribution functions for various near-Earth solar wind populations. The grey shaded region shows all solar wind in the interval 1998-2011. Coloured lines show subsets of these data: White, green, red and blue lines show uninverted, inverted, counterstreaming and undetermined HMF intervals, respectively.

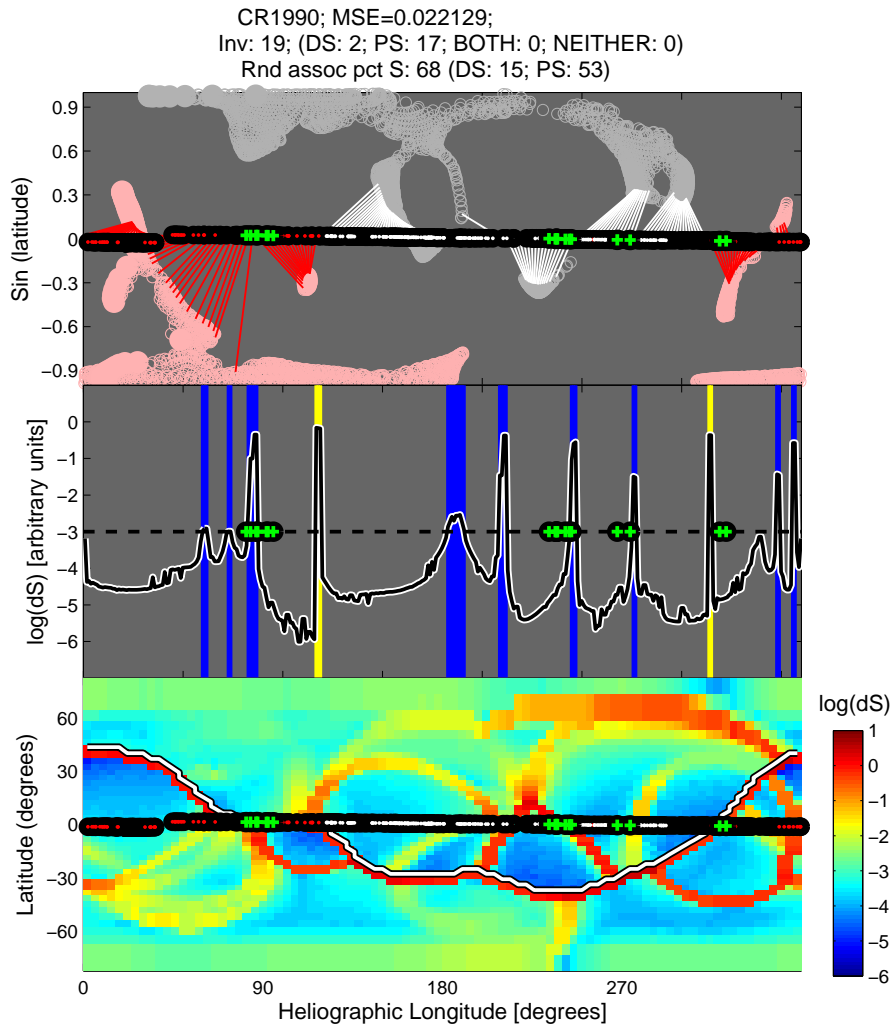


Figure 4. Top: A latitude-longitude map of the PFSS solution for Carrington rotation 1990. Pink/dark grey regions are the PFSS inward/outward coronal holes, with red/white lines showing the connection between the Earth’s orbit across the source surface and photosphere. Overlaid on the black strip are red/white dots showing the observed outward/inward sectors mapped to the source surface. Green crosses are inverted flux intervals. Middle: dS , photospheric foot point separation for adjacent points on the source surface, along the ecliptic plane (shown on a \log_e scale). This parameter serves as a means of identifying coronal streamers: Bipolar (pseudo) streamers are shown as vertical yellow (blue) lines. Bottom: contour plot of dS over all latitudes of the source surface. The HCS

is the white curve.

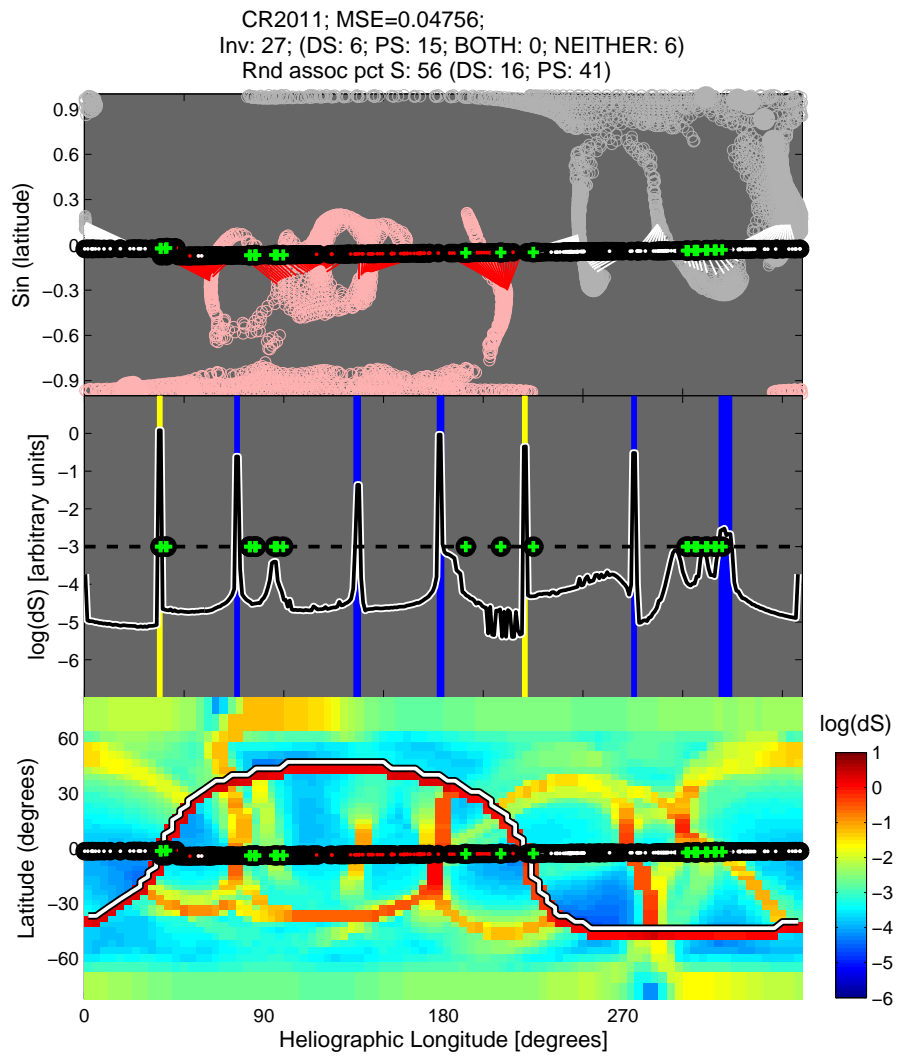
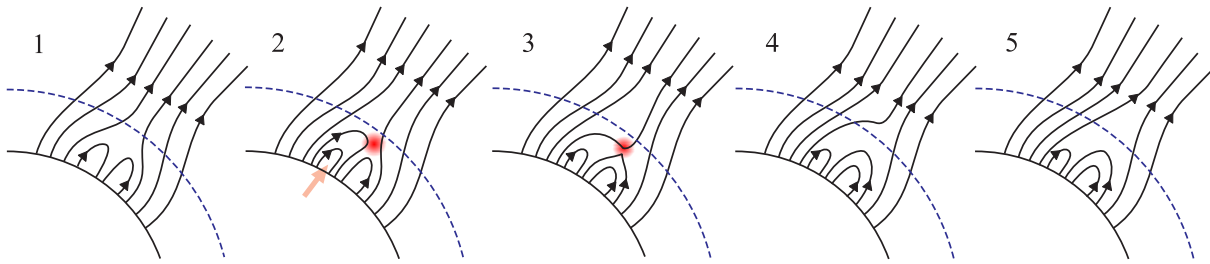


Figure 5. Parameters for Carrington rotation 2011, in the same format as Figure 4.

	Total	Any streamer	Pseudo (PS)	Bipolar (DS)	Both PS and DS	No streamer association
Inverted HMF	2263	1310	949	504	143	953
(% of total)	-	(57.9%)	(41.9%)	(22.3%)	(6.3%)	(42.1%)
Random interval	-	52.4%	39.0%	20.5%	5.1%	47.6%

Table 2. Solar origins of the inverted HMF intervals. Also shown is the probability that a random solar wind interval would be associated with the given type of streamer, *i.e.*, the percentage of ecliptic longitudes which are associated with different coronal structures.

(a) Pseudostreamer loop does not extend to solar wind formation height



(b) Pseudostreamer loop extends to solar wind formation height

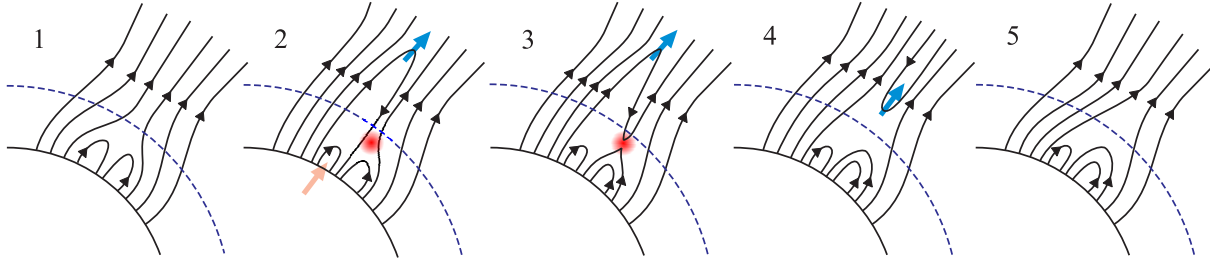


Figure 6. A sketch of interchange reconnection within a pseudostreamer. In the top panel, a closed loop rises due to photospheric flux emergence (red arrow), but does not reach the solar wind acceleration height (blue dashed line) before it undergoes reconnection with an open magnetic field line. This creates an Alfvén wave on the open magnetic field line which propagates out into the heliosphere, but does not create inverted HMF. The bottom panels show a loop which is dragged out by the solar wind (blue arrow) before interchange reconnection occurs. It does result in the creation of inverted HMF.